Influence of Surface Modification on the Acid Site Distribution of HZSM-5†

Shourong Zheng, Hilton R. Heydenrych, Andreas Jentys, and Johannes A. Lercher*

Technische Universität München, Institute for Chemical Technology, Lichtenbergstr. 4, D-85747 Garching, Germany

Received: November 8, 2001; In Final Form: May 2, 2002

Hydroxyl groups located on the external surface and in the pore mouth region of HZSM-5 zeolites with different crystal sizes were modified by chemical liquid deposition (CLD) of tetraethoxysilane (TEOS). The silylation of the acid sites was monitored using NH_3 sorption, IR spectroscopy of the zeolite hydroxyl groups, and adsorption of pyridine and di-*tert*-butyl-pyridine (DTBPy). Silylation reduced the concentration of Brønsted acid sites, preferentially in the pore mouth region of the zeolites, and led to a blocking of Lewis acid sites. The deactivation of Lewis acid sites was found to occur prior to the reaction with bridging hydroxyl groups and silanol groups. The efficiency of silylation achieved was found to depend on the particle size of the zeolite sample. A multicycle procedure can be used to increase the effects of the modification with TEOS.

Introduction

HZSM-5 zeolite has been extensively applied in many petrochemical processes[1,2] as its well-defined ten-membered ring channel system allows to achieve a high selectivity to *p*-isomers during disproportionation of alkyl-benzene, isomerization of dialkylbenzene and alkylation of toluene.[3−10] However, acid sites present on the external surface and in the pore mouth region of HZSM-5 zeolites usually lower the selectivity.[11−15]

Various modification methods have been applied to enhance the shape selectivity of HZSM-5 zeolites.[4,10−12,16−18] In general, the modifications aim at suppressing secondary reactions occurring on the external surface and/or at hindering the diffusion of undesired products out of the pores of the zeolites. Thus, the deactivation of the acid sites on the external surface (blocking active sites for secondary reactions) and/or the narrowing of the pore openings of HZSM-5 (enlarging differences in the diffusivities of isomers) improves the shape selectivity of HZSM-5 zeolites.

Post-synthesis modification by chemical vapor deposition (CVD) of silicon alkoxides, such as tetraethoxysilane (TEOS) and tetramethoxysilane (TMOS), is one of the most effective methods to enhance the shape selectivity of HZSM-5 zeolites. The silylation mechanism by means of CVD has been well documented by Niwa et al.[19−21] Because the minimum kinetic diameters of the silicon alkoxides typically used are larger than the pore diameter of HZSM-5, only hydroxyl groups on the outer surface and close to the pore openings react with the silylating agents and form Si−O−Si or Si−O−Al bonds, which leads to a passivation of these unselective acid sites. In addition, an inert silica layer is deposited on the outer surface and in the pore mouth region of the zeolites and, therefore, the pore openings are simultaneously narrowed or partially blocked.

Alternatively, chemical liquid deposition (CLD) can be used to modify the external surface of zeolites.[22−25] The main advantage of the reaction in liquid phase (CLD) compared to the reaction in gas-phase (CVD) is that the liquid reaction can be more easily transferred to an industrial preparation in large-scale quantities. However, systematic studies on the CLD mechanism, which allows a quantitative description of the modification effects, are lacking.

The concentration of acid sites in parent and modified zeolites has been extensively studied by pyridine adsorption and NH_3-TPD, as well as by test reactions, such as cracking of 1,3,4-triisopropylbenzene and *n*-hexane.[6,17,26] It should be emphasized, however, that these reports mostly address the qualitative changes induced by the surface modification. In a series of papers, O'Connor et al.[24−25,27] described the concentration of acid sites of silylated HZSM-5 zeolites by using TPD of 4-methyl-quinoline. As the kinetic diameter of 4-methyl-quinoline (0.73 nm) is larger than the pore openings of HZSM-5 zeolites (5.6 × 5.3 Å), this molecule is incapable of completely entering into the pores and, therefore, the passivation of the acid sites on the external surface of HZSM-5 by silylation can be quantitatively described. Recently, Melson et al.[28] used 2,4-dimethylpyridine adsorption to determine gravimetrically the concentration of acid sites on the external surface of HZSM-5. Corma et al.[29] studied the adsorption of di-*tert*-butyl-pyridine (DTBPy) by IR spectroscopy to quantitatively monitor externally accessible acid sites of different zeolites, such as mordenite, ZSM-5, ZSM-11, and SSZ-26, and Pieterse et al.[30] used IR spectroscopy to determine the concentration of the externally accessible acid sites of FER and TON zeolites by adsorption of 2,4,6-trimethylpyridine.

In this contribution, IR spectroscopy, NH_3-TPD and pyridine, as well as DTBPy adsorption, were used to quantitatively determine the changes in the concentration of externally accessible acid sites of HZSM-5 zeolites before and after CLD modification using TEOS. The quantitative results from different characterization methods are compared, and the mechanism of the modification is discussed on a molecular basis.

Experimental Section

Materials. Two samples of HZSM-5 with a Si/Al ratio of 45 (determined by X-ray fluorescence) and an average particle diameter of 0.5 and 3 μm (determined by SEM), designated HZS and HZL, were used as parent zeolites. X-ray diffraction

† Dedicated to Prof. J. Weitkamp on the occasion of his 60th birthday.
* Corresponding author.

10.1021/jp014091d CCC: $22.00
Published on Web 08/23/2002

(XRD) showed that HZL and HZS were highly crystalline materials and that the crystallinity of HZS was slightly lower compared to HZL. Pyridine and DTBPy were obtained from Sigma Aldrich. Hexane and tetraethoxysilane (TEOS, 99%) were obtained from Fluka. All chemicals were used as received.

Silylation. Typically, 2 g of zeolite was suspended in 50 mL of hexane and the mixture was heated under stirring until reflux. A 0.3 mL portion of TEOS, corresponding to a loading of 4 wt % SiO_2, was introduced into the mixture and the silylation was carried out for 1 h under reflux and stirring. Subsequently, hexane was removed by evacuation. The samples were dried at 393 K for 2 h and calcined at 773 K for 4 h in dry air. Samples prepared by single-cycle silylation are referred to as HZ×-4% (× denoting the zeolite with large or small crystals, 4% the concentration of SiO_2 deposited by wt %). Three-cycle silylation for HZS was carried out by repeating the above-described procedure, including the intermediate calcinations steps, for three times (the sample is referred to as HZS-3×4%).

^{27}Al MAS NMR. ^{27}Al MAS NMR spectra of the zeolites were recorded on a Bruker Avance MSL-300 NMR spectrometer at a field strength of 7.5 T and 15 kHz spinning speed using 4 mm ZrO_2 rotors. Spectra were collected at a frequency of 78.205 MHz with 1.0 μs excitation pulses and 0.1 s recycle times. The ^{27}Al chemical shifts were referenced to 1 M aqueous solution of $Al(NO_3)_3$.

NH_3 Sorption and Temperature Programmed Desorption. The NH_3 sorption and temperature programmed desorption (TPD) on the parent and silylated zeolites was studied using a modified SETARM TG-DSC 111 instrument. Around 15 mg of sample was pressed into wafers, broken into small platelets, and charged into the crucible of the TG-DSC system. The sample was activated by heating at 823 K for 1 h, and after cooling to 373 K NH_3 adsorption was carried out.

Physically adsorbed NH_3 was removed by degassing at 373 K until further weight loss was not observed (~3 h). NH_3-TPD of the sample was carried out by heating the sample at a rate of 10 K/min from 373 to 1073 K. The amount of NH_3 desorbed was quantitatively monitored by the weight loss and the partial pressure in the gas phase using a mass spectrometer.

IR Spectroscopy. The IR spectra were recorded at 4 cm^{-1} resolution using a Bruker IFS 88 FTIR spectrometer. The samples were pressed into self-supporting wafers and placed in a gold sample holder in the center of a furnace, which was mounted in an in situ cell connected to a vacuum system. The sample was activated in vacuum ($<10^{-6}$ mbar) by heating to 823 K at a rate of 10 K/min and held at this temperature for 1 h. All IR spectra were collected at 423 K. The adsorption of pyridine and DTBPy was carried out at a partial pressure of 2×10^{-2} mbar using an equilibration time of 15 min. After removing physically adsorbed molecules by degassing at 423 K for 1 h the IR spectra were collected at 423 K. To allow quantitative comparisons of the peak intensities, all IR spectra were normalized using the area of the overtone lattice vibration bands of the zeolites at 1990 cm^{-1} and 1870 cm^{-1}.

Note that the determination of the concentration of Brønsted acid sites accessible for DTBPy using the characteristic band at 3367 cm^{-1} was not possible for HZL and HZL-4% due to the low transmittance of these samples in the region of the hydroxyl groups. Therefore, the intensity of the characteristic band at 1616 cm^{-1} (characteristic of DTBPy adsorbed on Brønsted acid sites) and the results obtained from pyridine adsorption were used to quantitatively determine the concentration of accessible Brønsted acid sites. The intensities of the bridging hydroxyl groups of HZL and HZL-4% were obtained by eq 1:

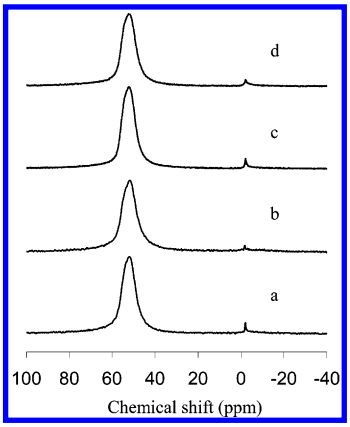

Figure 1. ^{27}Al MAS NMR spectra of (a) HZS, (b) HZS-3×4%, (c) HZL, and (d) HZL-4%.

$$A_{OH,L} = A_{OH,S} \times B_{Py,L}/B_{Py,S} \quad (1)$$

where $A_{OH,L}$ is the peak area of the bridging hydroxyl groups of the zeolite with the large crystal size, $A_{OH,S}$ is the peak area of the bridging hydroxyl groups of the zeolite with the small crystal size, $B_{Py,L}$ and $B_{Py,S}$ are the concentrations of Brønsted acid sites determined by pyridine adsorption on the zeolites with the large and small crystal sizes, respectively. The fractions of the bridging hydroxyl groups of HZL and HZL-4% interacting with DTBPy were obtained by:

$$A'_{OH,L} = A_{1616,L}/S_{1616,S} \quad (2)$$

where $A'_{OH,L}$ is the peak area of the bridging hydroxyl groups interacting with DTBPy for the sample with the large crystal size, $A_{1616,L}$ is the peak area of the band at 1616 cm^{-1}, and $S_{1616,S}$ is the slope of the linear relation between the area of the band at 1616 cm^{-1} and the amount of bridging hydroxyl groups interacting with DTBPy for the sample with the small crystal size.

Deuteration. Deuterium exchange of the zeolite was carried out under static conditions at 423 K and a D_2O partial pressure of 1mbar in the in situ IR cell. After activation at 823 K for 1 h, the zeolite was exchanged with D_2O for 40 min. The deuterium-exchanged zeolite was activated at 823 K to remove physically adsorbed D_2O, and the IR spectra were collected at 423 K.

Results

^{27}Al MAS NMR. The ^{27}Al MAS NMR spectra of the zeolites before and after silylation are compared in Figure 1. The ratios of extraframework Al species (EFAl) to framework Al species (FAl) calculated from the intensities of the peaks at a chemical shift of 0 ppm (octahedral Al) and 53 ppm (tetrahedral Al) were 0.024 and 0.028 for HZS and HZL, respectively, which indicates that for both samples the majority of Al is present in the framework of the zeolite. After silylation, the ratios of EFAl to EAl were slightly lowered to 0.020 and 0.022 for HZS-3×4% and HZL-4%.

IR Spectra of the Zeolites. The IR spectra of the activated HZS, HZS-4%, and HZS-3×4% samples are compared in Figure 2. The bands at 3745 cm^{-1}, 3606 cm^{-1}, and 3665 cm^{-1} are characteristic of isolated silanol groups located on the external surface of the zeolite, the bridging hydroxyl groups (Brønsted acid sites), and extraframework alumina species, respectively.[31]

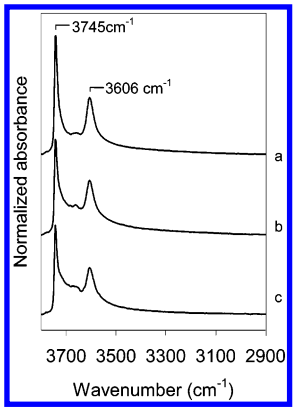

Figure 2. IR spectra of (a) HZS, (b) HZS-4%, and (c) HZS-3×4%.

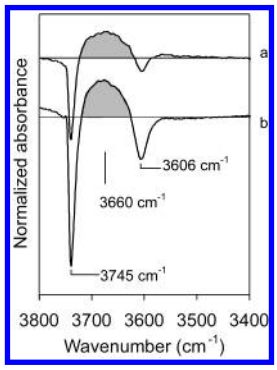

Figure 3. Changes in the IR spectra of activated (a) HZS-4% and (b) HZS-3×4% compared to HZS.

For HZL, the apparent transmittance at the region between 4000 and 2400 cm^{-1} was too low to obtain usable spectra.

To clearly visualize the changes in the hydroxyl group region of the spectra after modification, the differences of the IR spectra of HZS-4% and HZS-3×4% with that of HZS are shown in Figure 3. Two negative bands at 3745 and 3606 cm^{-1} and a new broad band with a maximum around 3660 cm^{-1} (indicated in gray) were observed. The presence of two negative bands at 3745 and 3606 cm^{-1} indicated that the concentration of the bridging hydroxyl and silanol groups decreased after silylation. The three-cycle silylation led to a further decrease in the concentration of the hydroxyl groups and to a further increase in the broad band (3660 cm^{-1}), which was assigned by Shaikh et al.[32] to hydrogen bonded silanol groups. To confirm this assignment, deuterium exchange was performed for HZS before and after silylation. The IR spectra of activated HZS, HZS-3×4%, deuterium-exchanged HZS, and deuterium-exchanged HZS-3×4% are shown in Figure 4. The bands partially remaining after deuteration of the zeolites at 3745 and 3606 cm^{-1} revealed that the isotope exchange was not complete for these hydroxyl groups.[33] It can be clearly seen, however, that all three hydroxyl bands appeared at the corresponding −O−D region, which clearly indicates that the broad band observed at 3660 cm^{-1} results from hydroxyl groups that are accessible for D_2O.

The changes in the intensity of the hydroxyl groups before and after modification are listed in Table 1. Single-cycle silylation for HZS led to a decrease in the concentration of the silanol and bridging hydroxyl groups by 6% and 9.5%, respectively. A further decrease in the concentration of these hydroxyl groups by 18% and 24% was observed after the three-cycle silylation, respectively. It is interesting to note that the ratios between the decrease in the concentration of the silanol and the bridging hydroxyl groups were almost the same after single- and three-cycle silylation.

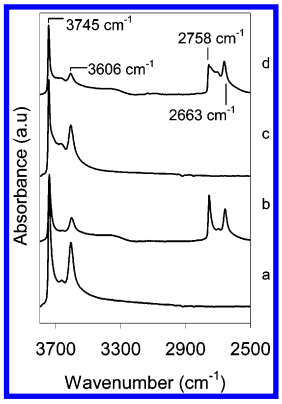

Figure 4. IR spectra of HZS after (a) activation and (b) deuterium exchange and HZS-3×4% after (c) activation and (d) deuterium exchange.

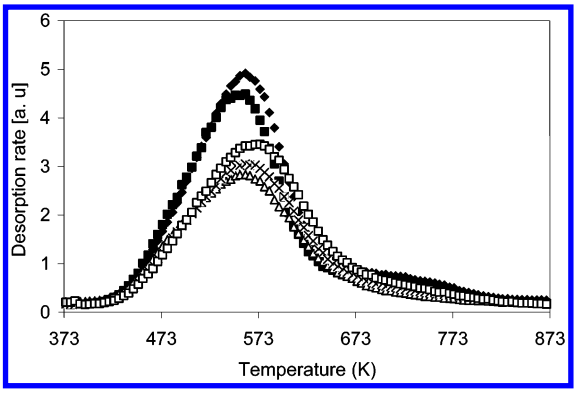

Figure 5. NH_3-TPD of (◆) HZL, (■) HZL-4%, (△) HZS-3×4%, (×) HZS-4%, and (□) HZS.

TABLE 1: Changes in the Concentration of Hydroxyl Groups after Silylation of HZS Compared to the Parent Material

	decrease of acid site concentration after modification (%)		ratio between 3745 cm^{-1} and 3610 cm^{-1}
sample	3745 cm^{-1}	3606 cm^{-1}	
HZS-4%	6	9.5	0.67
HZS-3×4%	18	24	0.75

TABLE 2: NH_3 Sorption Capacity of the Samples Investigated

sample	acid site density (mmol/g)	decrease of acid site concentration after modification (%)
HZS	0.304	
HZS-4%	0.275	9.5
HZS-3×4%	0.231	24
HZL	0.398	
HZL-4%	0.364	8.5

NH_3 Adsorption and Temperature Programmed Desorption. The NH_3-TPD and NH_3 uptakes of the parent and the silylated samples are shown in Figure 5 and summarized in Table 2, respectively. Only one desorption peak was observed in the NH_3-TPD of the parent and the modified zeolites, which is attributed to NH_3 desorption from Brønsted and strong Lewis acid sites. Note that NH_3 uptake for HZL was 33% higher compared to HZS, although the nominal Si/Al ratios were the same for both zeolites. This indicates that there is a larger amount of EFAl in HZS than in HZL. However, ^{27}Al MAS NMR did not indicate a markedly higher concentration of EFAl in the HZS sample, which is possibly due to the presence of NMR invisible EFAL resulting from the location of Al in nonsymmetric environments.[34−36] Single- and three-cycle silyl-

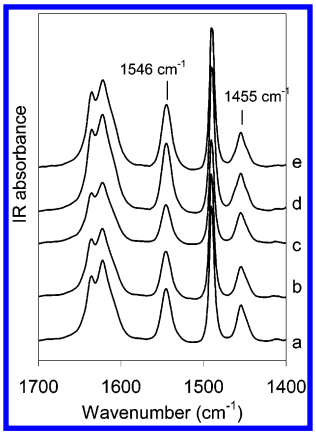

Figure 6. Changes in the IR spectra after adsorption of pyridine on (a) HZS, (b) HZS-4%, (c) HZS-3×4%, (d) HZL, and (e) HZL-4%.

TABLE 3: Concentration of Brønsted and Lewis Acid Sites Determined by Pyridine Adsorption

			decrease of acid site concentration after modification (%)	
sample	$c_{Brønsted}$ (mmol/g)	c_{Lewis} (mmol/g)	Brønsted	Lewis
HZS[a]	0.213	0.091		
HZS-4%	0.187	0.079	12	14
HZS-3×4%	0.154	0.079	28	14
HZL	0.280	0.107		
HZL-4%	0.261	0.095	6.7	13

[a] Concentration of the acid sites obtained from NH_3 adsorption.

ation for HZS led to a decrease in the concentration of acid sites by 9.5% and 24.0%, respectively. For HZL, silylation resulted in a decrease in the concentration of the acid sites by 8.5%.

Adsorption of Pyridine. The changes in the IR spectra after adsorption of pyridine on the zeolites before and after modification are compared in Figure 6. All samples investigated showed bands at 1636, 1491, and 1546 cm^{-1}, characteristic of pyridinium ions, and bands at 1623, 1490, and 1455 cm^{-1}, characteristic of coordinatively bound pyridine.[37] For the parent and silylated samples, the band at 3606 cm^{-1} completely disappeared after pyridine adsorption, which indicates that on all samples the acid sites are fully accessible for pyridine, and, furthermore, that silylation of the zeolites does not lead to a blockage of acid sites.

To quantify the acid sites of the parent and the silylated zeolites, the integral intensities of the bands at 1546 cm^{-1} (Brønsted acid sites) and 1455 cm^{-1} (Lewis acid sites), in combination with the total concentration of acid sites determined for HZS by NH_3-TPD, were used. The ratio between the molar extinction coefficients of the bands at 1455 and 1546 cm^{-1} was reported to be 1.5.[38] The concentration of Brønsted and Lewis acid sites is complied in Table 3.

Pyridine adsorption showed that single-cycle silylation of HZS and HZL led to a decrease in the concentration of Brønsted acid sites by 6.7% and 12.1%, respectively. Three-cycle silylation of HZS resulted in a decrease in the concentration of Brønsted acid sites by 27.5%. In addition, silylation also led to a decrease in the concentration of Lewis acid sites of HZS and HZL. It is interesting to note that single-cycle silylation for HZS deactivated the same amount of Lewis acid sites as three-cycle silylation.

Adsorption of Di-*tert*-butylpyridine. DTBPy was used as probe molecule to characterize acid sites located on the external surface and in the pore mouth region of the zeolites. As the

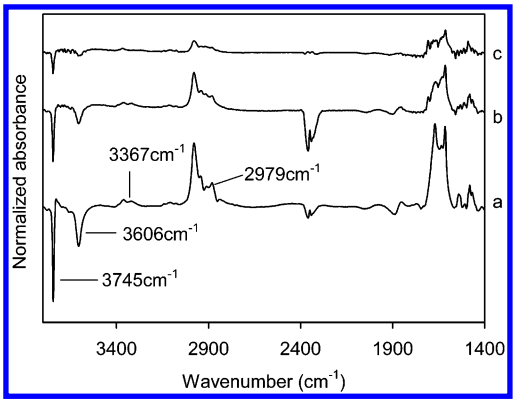

Figure 7. Changes in the IR spectra after adsorption of DTBPy on (a) HZS, (b) HZS-4%, and (c) HZS-3×4%.

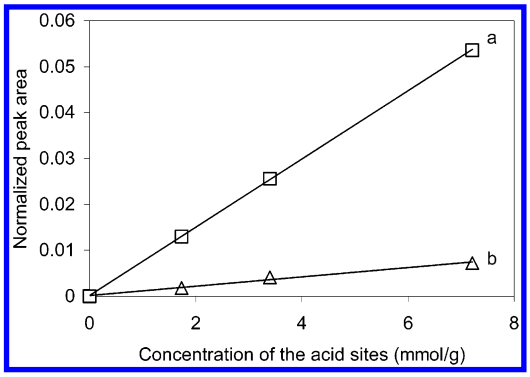

Figure 8. Correlation between concentration of acid sites interacting with DTBPy and area of the IR bands at (a) 3367 cm^{-1} and (b) 1616 cm^{-1}.

kinetic diameter of DTBPy (10.5 Å) is larger than the pore openings of HZSM-5 zeolites, DTBPy cannot penetrate into the pores of HZSM-5 zeolites and, therefore, DTBPy molecules can only interact with the hydroxyl groups on the external surface and in the pore mouth region of the zeolites.

The differences in the IR spectra after DTBPy adsorption on HZS, HZS-4%, and HZS-3×4%, and the activated samples, are shown in Figure 7. IR bands were observed at 3367, 2979, 2943, 2912, 2882, 1670, 1636, 1616, 1541, 1481, and 1468 cm^{-1}. The presence of two negative bands at 3745 and 3606 cm^{-1} indicate that DTBPy molecules interacted with silanol and bridging hydroxyl groups. The bands at 3367 and 1616 cm^{-1} were assigned to the N−H vibration and to the ring vibration of $DTBPyH^+$, respectively, and can be used to quantitatively assess the concentration of the externally accessible Brønsted acid sites.[29,39] The correlation between the concentration of Brønsted acid sites and the peak area of the bands at 3367 and 1616 cm^{-1} is shown in Figure 8. The linear relation indicates that the amount of DTBPy absorbed on the surface of the zeolites is proportional to the concentration of the bridging hydroxyl groups interacting with DTBPy.

The concentration of accessible hydroxyl groups is complied in Table 4. Approximately 28% of the bridging hydroxyl groups of HZS interacted with DTBPy. After single- and three-cycle silylation of HZS, 13% and 6.7% of the bridging hydroxyl groups remained accessible for DTBPy. For HZL, 7% of the acid sites interacted with DTBPy, while after silylation, only 2% of the acid sites were accessible for DTBPy. It is interesting to note that the ratios between the silanol groups and the bridging hydroxyl groups interacting with DTBPy remained almost constant after the different silylation cycles for HZS.

TABLE 4: Quantitative Results of DTBPy Adsorption

sample	bridging hydroxyl groups interacting with DTBPy (%)	ratio between silanol and bridging hydroxyl groups interacting with DTBPy	removal of acid sites (%)	removal of external acid sites (%)
HZS	28	0.78		
HZS-4%	13	0.83	15	53%
HZS-3×4%	6.7	0.75	22	76%
HZL	7.0			
HZL-4%	1.9		5.1	73%

Discussion

Surface Hydroxyl Groups. Three types of hydroxyl groups, i.e., silanol, bridging hydroxyl groups, and hydroxyl groups on nonframework aluminum oxide species, were observed for HZS. The silanol groups and some of the nonframework aluminum oxide species are located at or close to the external surface of the particles, while the location of the bridging hydroxyl groups remains still controversial. Frequently, it is argued that a fraction of the bridging hydroxyl groups are located on the external surface of HZSM-5 zeolites, which is attributed to the non-shape-selective behavior of the zeolites. On the other hand, Armaroli et al.[40] concluded that the bridging hydroxyl groups were only confined to internal pores of HZSM-5. In general, the zeolite surface is ill-defined and, therefore, the assignment whether acid sites are located on the external surface or not remains ambiguous. Note that probe molecules can also interact with acid sites located at the pore mouth of the zeolites, even if their dynamic diameter is larger than the pore openings.[30]

For the enhancement of the shape-selectivity by CVD or CLD, knowledge about the distribution of the bridging hydroxyl groups on the external surface and in the pore mouth of HZSM-5 zeolites is essential. The first step of silylation is assumed to be initiated on the bridging hydroxyl groups accessible for the silylating agent.[19] Conceptually, the enhancement of the shape selectivity by silylation results from the passivation of nonselective acid sites and, in parallel, from the narrowing of the pore openings of the zeolites.[20−22] Note that the narrowing of the pore openings would be most effectively achieved if the bridging hydroxyl groups were located in the pore mouth, while only a minor narrowing of the pore openings would be expected if silylation occurs on the external surface of the zeolite crystals only. We have observed that a more effective pore mouth narrowing has been achieved by CLD of tetramethoxysilane (TMOS) compared to TEOS.[41] As the critical diameter of TMOS (8.9 Å) is smaller than that of TEOS (10.3 Å), TMOS molecules could reach deeper into the pores of the zeolite. These results indicate that the silylation mainly occurs at the pore mouth of the zeolite and that most of the bridging hydroxyl groups are located in the pores of zeolites, which is in agreement with the results of Armaroli et al.[40]

After silylation by CLD, the formation of new hydroxyl groups was observed. The shift of the O−H stretching frequency to a lower wavenumber and the broadening of the band indicate that location and geometric environment of these hydroxyl groups are different from silanol groups on the external surface. As silylation is expected to occur in the pore mouth region, we speculate that the newly formed silanol groups are also located in the pore mouth region and, furthermore, that the geometry of the pores leads to the formation of hydrogen bonding interactions between these silanol groups. The increase in the intensity of this broad band and the simultaneous narrowing of the pores of the zeolite also confirms that the newly formed silanol groups are located in a sterically constrained region, i.e., the pore mouth region of the zeolites.[41]

Acid Sites on the External Surface and in the Pore Mouth of the Zeolites. As the diameter of TEOS is larger than that of the pores of HZSM-5 zeolite, silylation by CLD of TEOS only modifies the external surface and the pore mouth of HZSM-5 zeolites.[42] The decrease in the concentration of the hydroxyl groups of the zeolites after silylation by CLD was unequivocally determined using different characterization methods. Approximately 7.0% and 28% of the bridging hydroxyl groups were accessible for DTBPy in HZL and HZS, respectively, which is attributed to the different particle size of the two parent materials. As the specific surface area of spherical particles is reciprocally proportional to their radius, the specific surface area of the outer surface should be approximately six times larger for HZS compared to HZL. However, the fraction of acid sites located on the external surface and in the pore mouth region of HZS was found to be only four times higher than that of HZL. The difference can be tentatively attributed to (i) a lower concentration of the acid sites on the external surface and in the pore mouth region of HZS, or (ii) a narrowing of the pore entrance of HZS by EFAl. One should note that there is a larger amount of EFAl present in HZS compared to HZL, which might narrow the pores of HZS and, thus, constrains the DTBPy sorption on accessible Brønsted acid sites.

For both samples, silylation also led to a decrease in the concentration of Lewis acid sites as already described by Shaikh et al.[32] For HZS, single-cycle and three-cycle silylation led almost to the same decrease in the concentration of Lewis acid sites, which indicates that all Lewis acid sites accessible for TEOS are already completely silylated after the first cycle. This points to an easier accessibility of the Lewis acid sites located on aluminum oxide species and suggests that the silylation of Lewis acid sites proceeds more rapidly than that of Brønsted acid sites.

For single-cycle silylation, pyridine adsorption showed that 0.038 mmol/g of the acid sites (Brønsted acid sites + Lewis acid sites) of HZS and 0.031 mmol/g of the acid sites of HZL were passivated. Considering the significantly higher concentration of acid sites accessible for TEOS on HZS and that an excess of TEOS was used in each cycle, we conclude that a higher efficiency for silylation was achieved for the sample with the larger particle size. In contrast, multiple silylation cycles were necessary for HZS, however, they did not lead to the same fractional decrease in the concentration of acid sites for each cycle. Note that the first silylation cycle of HZS led to a removal of 53% of the acid sites on the external surface and in the pore mouth region, while during the subsequent cycles only 76% of the acid sites were passivated, although a significant amount of acid sites remained in the pore mouth region. This might indicate that the acid sites on the external surface and in the pore mouth region were not homogeneously distributed.

During the first silylation cycle, we conclude that TEOS molecules react with accessible acid sites and attach to the surface of the zeolite. This may hinder other TEOS molecules to access vicinal acid sites, if the concentration of the acid sites

is high. The acid sites, however, may become accessible during subsequent silylation cycles, because the bulky ethoxyl groups on TEOS are removed during the calcination. Thus the density of the acid sites strongly affects the extent of the silylation reaction. As the Si/Al ratios of the zeolites used were relatively high (i.e., 45), the distribution of the acid sites should have only a minor influence on the passivation effects. Therefore, we would like to assign the different silylation effects to acid sites located at different depths in the pores of the zeolite. During the first silylation cycle, TEOS molecules preferentially interact with acid sites that are easily accessible and, therefore, high passivation effects are achieved. In the second and third cycle, the concentration of accessible acid sites is strongly reduced and the narrowing of the pore openings further hinders TEOS molecules from penetrating into zeolite pores. Therefore, a decreasing extent of passivation can be expected in subsequent modification cycles.

Silylation Mechanism in CLD. The concentration of silanol groups, bridging hydroxyl groups, and Lewis acid sites was reduced after silylation by TEOS. Niwa et al.[19,32,43] proposed, based on the acid strength of different hydroxyl groups, that the reactivity of the bridging hydroxyl groups was higher than that of the silanol groups. In addition, CVD modification of aluminum oxide indicated that at first a homogeneous monolayer of silica was generated before the first Si−O−Si bonds were formed. It was also found that silylation of silicalite and NaZSM-5 zeolites is less effective compared to silylation of acidic zeolites.[44,45] Combining these results, the reactivity of the three sites should be: Lewis acid sites ∼ bridging hydroxyl groups > silanol groups.

For HZS, all accessible Lewis acid sites for TEOS were removed by silylation, while in contrast, multicycle silylation led to a further decrease in the concentration of the silanol and the bridging hydroxyl groups. This suggests that the reaction of TEOS with Lewis acid sites occurs prior to the silanol and the bridging hydroxyl groups, because a fraction of Lewis acid sites are located at the external surface, thus, having a higher accessibility for TEOS compared to the bridging hydroxyl groups, and additionally, Lewis acid sites are probably stronger acidic than Brønsted acid sites. For each silylation cycle, a decrease in the concentration of the silanol groups was observed before the complete deactivation of the accessible bridging hydroxyl groups, although the reactivity of the bridging hydroxyl groups with TEOS is higher than the silanol groups. This suggests that TEOS molecules react with the bridging hydroxyl groups and subsequently condense with vicinal silanol groups during calcination. The similar ratio of the decrease in the concentration of the silanol and bridging hydroxyl groups for single and multicycle silanization confirms this.

The CLD mechanism of the silylation process is shown in Scheme 1. Silylation of the zeolites includes two stages (i) the liquid phase reaction and (ii) the calcination process. The hydrolysis of TEOS only occurs on Brønsted and Lewis acid sites during the liquid-phase reaction, which leads to the formation of Si−O−Al bonds. During calcination, the residual ethoxyl groups are oxidized into hydroxyl groups, which partially condense with vicinal silanol groups to form Si−O−Si bands. Therefore, modification of zeolites by CLD of TEOS leads to a simultaneous decrease in the concentration of Brønsted sites, Lewis acid sites, and silanol groups.

In general, modification of zeolites with different crystal sizes will lead to different silylation effects. Zeolites with small crystals and a high specific surface area require a comparatively high amount of silylating agent and, in most cases, multicycle

SCHEME 1: Scheme of Silylation Reaction between TEOS and the Surface Hydroxyl Groups of HZSM-5

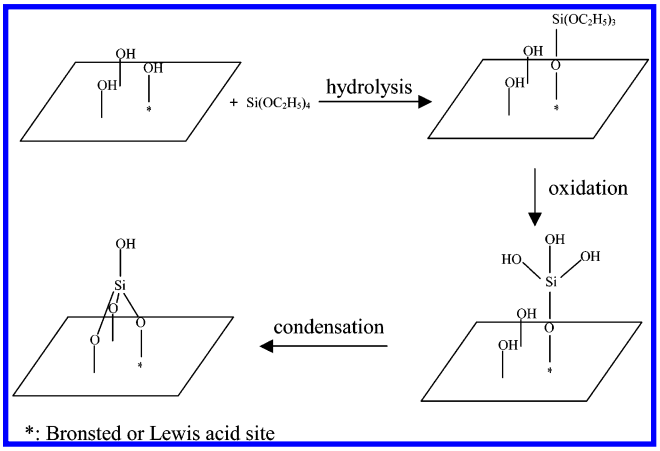

silylation to achieve an effective passivation of unselective acid sites. The presence of EFAl also lowers the silylation efficiency. Typically, zeolites with small crystal size contain a relatively high amount of EFAl because of the fast crystallization. Therefore, pretreatment of zeolites, such as pre-dealumination of the external surface of zeolites, [41] can be used to enhance the modification effects.

Conclusions

Silylation of HZSM-5 with CLD of TEOS leads to the passivation of Brønsted and Lewis acid sites on the external surface and in the pore mouth region of the zeolites. For samples with small crystal sizes, single-cycle silylation deactivates all Lewis acid sites accessible for TEOS; however, a multicycle silylation is advantageous to further deactivate Brønsted acid sites. In contrast, for samples with large crystals, effective silylation can be achieved with a single-cycle silylation step. The deactivation of Lewis acid sites occurs prior to the passivation of Brønsted acid sites and silanol groups, which results from the easier accessibility and higher acid strength of Lewis acid sites. The deactivation of the Brønsted acid sites is attributed to a hydrolysis reaction with TEOS, while the reaction with the silanol groups occurs during the subsequent calcination by a condensation of the hydroxyl groups.

Silylation preferentially occurs in the pore mouth region. New hydrogen bonded hydroxyl groups are formed by CLD modification in the pore mouth region of the zeolite.

Acknowledgment. The authors thank J.-O. Barth for the measurements of the ^{27}Al MAS NMR. Financial support from the Bayerische Forschungsverbund Katalyse (FORKAT II) and Süd-Chemie AG is gratefully acknowledged.

References and Notes

(1) Weitkamp, J. *Solid State Ionics* **2000**, *131*, 175.
(2) Kaeding, W. W.; Barile, G. C.; Wu, M. M. *Catal. Rev.-Sci. Eng.* **1984**, *26*, 597.
(3) Olson, D. H.; Haag, W. O. *Catalytic Materials*, ACS Symposium Series, Vol. 248, American Chemical Society: Washington, DC, 1984.
(4) Kaeding, W. W.; Chu, C.; Young, L. B.; Weinstein, B.; Butter, S. A. *J. Catal.* **1981**, *67*, 159.
(5) Das, J.; Bhat, Y. S.; Halgeri, A. B. *Ind. Eng. Chem. Res.* **1994**, *33*, 246.
(6) Röger, H. P.; Krämer, M.; Möller, K. P.; O'Connor, C. T. *Microporous Mesoporous Mater.* **1998**, *21*, 607.
(7) Mirth, G.; Lercher, J. A. *J. Catal.* **1991**, *95*, 3736.
(8) Mirth, G.; Cejka, J.; Lercher, J. A. *J. Catal.* **1993**, *139*, 24.
(9) Mirth, G.; Lercher, J. A. *J. Catal.* **1994**, *147*, 199.
(10) Hibino, T.; Niwa, M.; Murakami, Y. *J. Catal.* **1991**, *128*, 551.

(11) Kürschner, U.; Jerschkewitz, H. G.; Schreier, E.; Völter, *Appl. Catal.* **1990**, *57*, 167.
(12) Wang, I.; Ay, C. L.; Lee, B. J.; Chen, M. H. *Appl. Catal.* **1989**, *54*, 257.
(13) Bhat, Y. S.; Das, J. Rao, K. V.; Halgeri, A. B. *J. Catal.* **1996**, *159*, 368.
(14) Fraenkel, D. *Ind. Eng. Chem. Res.* **1990**, *29*, 1814.
(15) Csicsery, S. M. *Zeolites* **1984**, *4*, 202.
(16) Kaeding, W. W.; Chu, C.; Young, L. B.; Butter, S. A. *J. Catal.* **1981**, *69*, 392.
(17) Tynjala, P.; Pakkanen, T. T. *J. Mol. Catal. A* **1997**, *122*, 159.
(18) Fang, L. Y.; Liu, S. B.; Wang, I. *J. Catal.* **1999**, *185*, 33.
(19) Niwa, M.; Katada, N.; Murakami, T. *J. Phys. Chem.* **1990**, *94*, 6441.
(20) Niwa, M.; Kanada, N.; Murakami, Y. *J. Catal.* **1992**, *134*, 340.
(21) Niwa, M.; Kato, S.; Hattori, T.; Murakami, Y. *J. Chem. Soc., Faraday Trans. 1* **1984**, *80*, 3135.
(22) Yue, Y. H.; Tang, Y.; Liu, Y.; Gao, Z. *Ind. Eng. Chem. Res.* **1996**, *35*, 430.
(23) Gründling, C.; Eder-Mirth, G.; Lercher, J. A. *J. Catal.* **1996**, *160*, 299.
(24) Weber, R. W.; Möller, K. P.; Unger, M.; O'Conner, C. T. *Microporous Mesoporous Mater.* **1998**, *23*, 179.
(25) Weber, R. W.; Möller, K. P.; O'Conner, C. T. *Microporous Mesoporous Mater.* **2000**, *35*, 533.
(26) Kim, J. H.; Ishida, A.; Okajima, M.; Niwa, M. *J. Catal.* **1996**, *161*, 387.
(27) Weber, R. W.; Fletcher, J. C. Q.; Möller, K. P.; O'Conner, C. T. *Microporous Mater.* **1996**, *7*, 15.
(28) Melson, S.; Schüth, F. *J. Catal.* **1997**, *170*, 46.
(29) Coma, A.; Fornes, V.; Forni, L.; Marquez, F.; Martinez-Triguero, J.; Moscotti, D. *J. Catal.* **1998**, *179*, 451.
(30) Pieterse, J. A. Z.; Veefkind-Reyes, S.; Seshan, K.; Lercher, J. A. *J. Phys. Chem. B* **2000**, *104*, 5715.
(31) Sayed, M. B.; Kydd, R. A.; Cooney, R. P. *J. Catal.* **1984**, *88*, 137.
(32) Shaikh, R. A.; Hegde, S. G.; Behlekar, A. A.; Rao, B. S. *Catal. Today* **1999**, *49*, 201.
(33) Vimont, A.; Thibault-Starzyk, F.; Lavalley, J. C. *J. Phys. Chem. B* **2000**, *104*, 286.
(34) Man, P. P.; Klinowski, J. *Chem. Phys. Lett.* **1988**, 147, 581.
(35) Brunner, E.; Ernst, H.; Freude, D.; Frohlich, T.; Hunger, M.; Pfeifer, H. *Stud. Surf. Sci. Catal.* **1989**, 49A, 623.
(36) Grobet, P. J.; Geerts, H.; Tielen, M.; Martens, J. A.; Jacobs, P. A. *Stud. Surf. Sci. Catal.* **1989**, 46, 721.
(37) Glazunov, V. P.; Odinokov, S. E. *Spectrochim. Acta* **1982**, 38A, 399.
(38) Emeis, C. A. *J. Catal.* **1993**, *141*, 347.
(39) Knözinger, H.; Krietenbrink, H.; Ratnasamy, P. *J. Catal.* **1977**, *48*, 436.
(40) Armaroli, T.; Trombetta, M.; Alejandre, A. G.; Solis, J. R.; Busca, G. *Phys. Chem. Chem. Phys.* **2000**, *2*, 3341.
(41) Zheng, S.; Heydenrych, H. R.; Jentys, A.; Lercher, J. A. *Top. Catal.*, submitted.
(42) Zheng, S.; Heydenrych, H.; Röger, P.; Jentys, A.; Lercher, J. A. *Stud. Surf. Sci. Catal.* **2001**, *135*, 214.
(43) Hibino, T.; Niwa, M.; Murakami, Y. *Zeolites* **1993**, 13, 519.
(44) Begum, H. A.; Katada, N.; Niwa, M. *Microporous Mesoporous Mater.* **2001**, *46*, 13.
(45) Chun, Y.; XU, Q.; Yan, A.; Ye, X. *Stud. Surf. Sci. Catal.* **1997**, *105*, 2075.